



1 **Contributions of Transparent Exopolymer Particles by**
2 **Specific Phytoplankton Groups in the Cosmonaut Sea, East**
3 **Antarctic**

4 Ji Hu^{1, &}, Siyou Xue^{2, &}, Jun Zhao^{1, *}, Dong Li¹, Gaojing Fan³, Peisong Yu^{1, *}, Haifeng
5 Zhang¹, Changfeng Zhu¹, Keyu Tao¹, Xufeng Yang¹, Cai Zhang¹, Jianmin Pan¹, Min
6 Chen²

7 ¹Key Laboratory of Marine Ecosystem Dynamics, Second Institute of Oceanography, Ministry of Natural
8 Resources, Hangzhou 310012, China

9 ²College of Ocean and Earth Sciences, Xiamen University, Xiamen 361102, China

10 ³Polar Research Institute of China, Shanghai 200136, China

11 ^{*}Correspondence to: Zhao Jun (jzhao@sio.org.cn); Yu Peisong (yuppe@sio.org.cn).

12 [&]These authors contributed equally to this work and should be considered co-first authors.



Abstract: Transparent exopolymer particles (TEP) play a crucial role in marine carbon cycling. While phytoplankton are known to be the primary contributors to TEP, the impact of changes in phytoplankton community structure on TEP production in natural aquatic environments remains incompletely understood. This study employed multiple linear regression (MLR) modeling to quantify the contributions of two dominant phytoplankton groups, diatoms and haptophytes (primarily *Phaeocystis antarctica*), to TEP production in the surface waters of the Cosmonaut Sea, antarctica during the austral summer. Results demonstrate that in situ TEP production by each group can be estimated by scaling laboratory-derived theoretical values with an environmentally adjusted correction factor (β). These β factors, primarily governed by phytoplankton community structure, reveal taxon-specific discrepancies between field and laboratory TEP production capacities. Notably, temperature, ammonium, and polysaccharide composition act as secondary modifiers of β through indirect physiological effects. This study revealed that when the chlorophyll *a* concentration (Chl *a*) of *P. antarctica* exceeds 0.5 $\mu\text{g/L}$ in the Cosmonaut Sea, its TEP production capacity surpasses that of diatoms at equivalent biomass levels—challenging the paradigm of diatom-dominated TEP contributions. In the research area, *P. antarctica* contributed 14.6 – 82.5% (mean: $48.6 \pm 15.4\%$) to total TEP production, while diatoms contributed 31.0 – 112.0% (mean: $55.1 \pm 21.2\%$; values $>100\%$ reflect co-occurring group contributions). This highlights the pivotal role of *P. antarctica* in Southern Ocean carbon cycling and provides mechanistic insights for refining polar carbon budget models.

Keywords: Transparent exopolymer particles, *Phaeocystis antarctica*, Multiple linear regression modeling, Cosmonaut Sea

1 Introduction

Transparent exopolymer particles (TEP), predominantly composed of high-molecular-weight acidic polysaccharides, are a significant component of marine organic matter (Passow, 2002a; Passow, 2002b; Zhou et al., 1998). These gel-like polymers play a crucial role in marine carbon cycling due to their distinctive physicochemical properties, such as high viscosity (Mopper et al., 1995), low density (Engel and Schartau, 1999; Azetsu-Scott and Passow, 2004), and substantial carbon content (Smith et al., 1995). Phytoplankton serve as the primary source of TEP in marine ecosystems (Aluwihare and Repeta, 1999; Radic et al., 2005; Fukao et al., 2010). Numerous studies have documented TEP production across diverse algal taxa, with



40 notable contributions from diatoms (Passow and Alldredge, 1994), flagellates (Passow, 2002a; Guo et al.,
41 2022), coccolithophores (Engel et al., 2002), and *Phaeocystis* spp. (Hong et al., 1997; Ramaiah et al., 2001).
42 Diatoms, in particular, have been consistently identified as the most prolific TEP producers (Engel, 1998;
43 Passow, 2002b; Passow, 2002a; Engel, 2004), with phytoplankton-derived polysaccharides accounting for
44 70-94 % of the extracellular organic carbon pool (Biddanda and Benner, 1997). However, the quantitative
45 contribution of different phytoplankton species to TEP production exhibits considerable variability,
46 influenced by species-specific metabolic traits, physiological status, and ambient environmental conditions
47 (Penna et al., 1999; Staats et al., 2000).

48 TEP production occurs throughout the various growth phases of phytoplankton, including exponential,
49 stationary, and senescent stages (Fukao et al., 2010). Significant interspecies variability in TEP production
50 capacity has been documented, attributed to differences in growth rates among phytoplankton species (Waite
51 et al., 1995; Engel, 1998; Passow, 2002a). Several environmental parameters regulate TEP production
52 through their effects on phytoplankton, including: (1) light intensity (Hong et al., 1997), (2) CO₂
53 concentration (Engel, 2002), (3) temperature (Guo et al., 2022), and (4) nutrient and trace metal availability
54 (Kraus, 1997). Additionally, physical factors such as turbulence significantly influence TEP formation
55 dynamics (Passow, 2000). Empirical studies have established exponential relationships between chlorophyll-
56 a (Chl *a*) concentrations and TEP production for specific phytoplankton taxa (Passow and Alldredge, 1995a;
57 Waite et al., 1995; Hong et al., 1997; Passow, 2002a). However, these models are primarily derived from
58 laboratory monoculture experiments or single-species field investigations, while natural marine ecosystems
59 feature complex, multi-species phytoplankton assemblages. Despite significant advances in understanding
60 the environmental controls on TEP production, key gaps remain regarding species-specific TEP production
61 in mixed phytoplankton communities and interactions among coexisting phytoplankton groups. To address
62 these limitations, this study aims to develop a novel methodology to quantify the relative contributions of
63 diverse phytoplankton groups to TEP production in marine ecosystems.

64 Multiple linear regression (MLR) is a robust statistical method for modeling linear relationships between
65 multiple independent variables and a single dependent variable (DeVore and Kaukis, 2003; Montgomery et
66 al., 2021). This approach is theoretically appropriate for analyzing the association between phytoplankton-



67 derived TEP (independent variables) and measured TEP concentrations (dependent variable), given the
68 established role of phytoplankton as primary TEP producers. However, the application of MLR becomes
69 problematic in coastal ecosystems that receive substantial terrestrial inputs, such as riverine discharges and
70 continental shelf exchanges (Li et al., 2018; Ge et al., 2022). In these environments, allochthonous organic
71 matter may constitute a significant portion of TEP pools, challenging the conventional assumption of
72 phytoplankton dominance in TEP production. Consequently, MLR exhibits limited applicability for fitting
73 TEP data in such environments.

74 The Southern Ocean is a critical component of the global carbon cycle and ranks among the largest oceanic
75 carbon sinks globally (Arteaga et al., 2018). In this region, autochthonous production by phytoplankton is
76 the primary source of organic matter (Arrigo et al., 2008; Arrigo et al., 2015; Lee et al., 2017; Ortega-Retuerta
77 et al., 2017). The Cosmonaut Sea, in particular, features a relatively simple phytoplankton community
78 structure, predominantly consisting of *Phaeocystis antarctica* (*P. antarctica*) and diatoms (Li et al., 2024).
79 This simplified ecosystem is sustained by unique hydrographic conditions, where sea-ice dynamics and water
80 mass properties promote strong vertical stratification and exceptional environmental stability in surface
81 waters (Williams et al., 2010). These distinctive characteristics collectively establish the Cosmonaut Sea an
82 ideal natural laboratory for studying phytoplankton dynamics and their role in carbon sequestration.

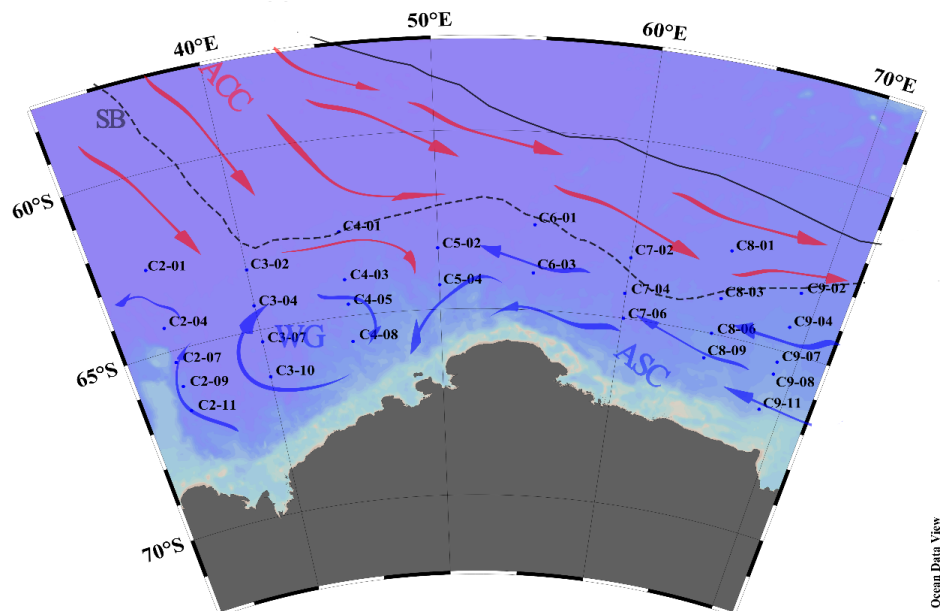
83 This study analyzes TEP and phytoplankton pigment samples collected from the surface layer of the
84 Cosmonaut Sea during the 36th Chinese National Antarctic Research Expedition. By employing MLR
85 modeling on these in situ measurements, we quantitatively evaluate the relative contributions of different
86 phytoplankton functional groups to TEP production in this environmentally homogeneous region. Our
87 investigation focuses on two primary objectives: (1) to resolve a critical gap in understanding the
88 biogeochemical cycling of TEP in Southern Ocean ecosystems by isolating community-structure controls,
89 and (2) to advance the mechanistic understanding of phytoplankton ecological roles in carbon export by
90 establishing direct connections between plankton composition and TEP-driven organic matter production.
91 The findings demonstrate that phytoplankton community structure is the principal regulator of TEP dynamics
92 in this climatically sensitive region, providing a framework for scaling group-specific carbon fluxes.



93 **2 Materials and methods**

94 **2.1 Sampling stations**

95 This study utilized samples collected from the Cosmonaut Sea in East Antarctica during the 36th Chinese
96 Antarctic Research Expedition (CHINARE-36). The sampling locations are illustrated in Figure 1, with
97 detailed information provided in Table 1. Sampling was conducted in surface seawater from December 8,
98 2019, to January 6, 2020, within the coordinates of 60 °S, 34.97 °E to 70 °S, 70.00 °E. Basic hydrological
99 parameters were obtained using a Sea-Bird SBE 911 CTD. Water samples were collected using a 10 L Niskin
100 bottle. The parameters measured included water temperature, salinity, water depth, photosynthetically active
101 radiation (PAR), nutrients, TEP, and pigments, as detailed in Section 2.2. Furthermore, the study area is
102 influenced by two major current systems: the eastward-flowing Antarctic Circumpolar Current (ACC) and
103 the westward-flowing Antarctic Slope Current (ASC). Specifically, the region west of Cape Ann is affected
104 by the eastern Weddell Gyre (WG) (Williams et al., 2010).



105 **Figure 1: Sampling stations in the Cosmonaut Sea (ACC: Antarctic Circumpolar Current; ASC: Antarctic Slope**
106 **Current; SB: Southern Boundary; WG: Weddell Gyre)**



109

110

111 **Table 1 Detailed information of surface sampling stations in the Cosmonaut Sea**

Station	Date	Longitude (°E)	Latitude (°N)	Sampling depths (m)	Sea ice
C4-01	2019/12/24	45.00	-62.65	0	No
C4-03	2019/12/25	44.98	-63.99	0	No
C4-05	2019/12/25	45.01	-64.68	0	No
C4-08	2019/12/26	45.00	-65.70	0	No
C3-10	2019/12/27	40.00	-66.31	0	No
C3-07	2019/12/28	39.99	-65.33	0	No
C3-04	2019/12/29	39.97	-64.32	0	No
C3-02	2019/12/31	40.01	-63.31	0	No
C2-01	2020/1/1	35.01	-62.66	0	No
C2-04	2020/1/2	34.98	-64.34	0	No
C2-07	2020/1/5	35.03	-65.33	0	No
C2-09	2020/1/6	34.99	-66.01	0	No
C2-11	2020/1/6	35.01	-66.69	0	No
C6-01	2019/12/21	54.94	-62.64	0	No
C6-03	2019/12/22	54.99	-63.98	0	No
C5-04	2019/12/23	50.00	-64.33	0	No
C5-02	2019/12/23	49.98	-63.31	0	No
C9-07	2019/12/8	68.94	-65.32	0	No
C9-08	2019/12/8	68.95	-65.66	0	No
C9-11	2019/12/9	68.79	-66.68	0	No
C9-04	2019/12/11	69.00	-64.32	0	No
C9-02	2019/12/12	69.03	-63.32	0	No
C8-01	2019/12/13	65.00	-62.65	0	No
C8-03	2019/12/14	65.04	-64.01	0	No
C8-06	2019/12/16	65.00	-65.00	0	No
C8-09	2019/12/16	64.91	-65.69	0	No
C7-06	2019/12/18	60.08	-65.00	0	Yes
C7-04	2019/12/19	59.95	-64.31	0	No
C7-02	2019/12/20	59.99	-63.32	0	No

Note: Sea ice concentration data were obtained from remote sensing observations provided by the University of Bremen (available at: <https://data.seaice.uni-bremen.de/databrowser/>). Of all the sampling stations, only station C7-06 exhibited the presence of sea ice, while all other stations were free of ice during the investigation period.

112 2.2 Parameter determination



113 **2.2.1 Basic parameters**

114 Hydrological parameters including temperature, salinity, and water depth were measured using a Sea-Bird
115 SBE 911 Plus CTD. PAR data were obtained from a PAR sensor integrated with the CTD system.

116 **2.2.2 Nutrients**

117 Seawater samples were filtered through 0.45 μm acetate fiber membranes and subsequently stored at -20 $^{\circ}\text{C}$
118 until analysis. Nutrient determinations were conducted in accordance with the 'Marine Survey Specification
119 GB/T 12763.4'. Ammonium concentrations were measured on-site using a 7230G spectrophotometer, while
120 the remaining four nutrients were analyzed using a continuous flow nutrient automatic analyzer (Skalar
121 San++, Netherlands). The standard solutions used for analysis were obtained from the Reference Material
122 Center of the Second Institute of Oceanography, Ministry of Natural Resources (GBW 08617-08645). The
123 precision of the measurements for ammonium, nitrate, phosphate, and silicate were 1.2 %, 2.4 %, 2.4 %, and
124 3.0 %, respectively.

125 **2.2.3 TEP**

126 The method for determining TEP primarily follows the experimental protocol established by Passow and
127 Alldredge (1995b). Approximately 100 mL of seawater samples were collected and filtered through a 25 mm
128 diameter polycarbonate filter membrane with a pore size of 0.4 μm , using a negative pressure of less than
129 0.02 MPa. Subsequently, 500 μL of 0.02 % Alcian blue (8 GX, pH = 2.5, Sigma) was added for staining,
130 ensuring that the membrane surface was fully immersed for 2 seconds. Excess dye was removed by washing
131 the membrane with deionized water. The membrane sample was then dissolved in 6 mL of 80 % sulfuric acid
132 for 2 hours, during which the test tube was manually agitated 3 to 5 times. Finally, the supernatant was
133 transferred to a 1 cm cuvette, and the absorbance was measured at a wavelength of 787 nm. Each surface
134 station was sampled 2 to 3 times, and the average absorbance value was recorded after subtracting the blank
135 reading from the filter membrane.

136 The absorbance values were determined using an enhanced calibration method for xanthan gum, as described
137 by Bittar et al. (2018). Initially, a series of xanthan gum standard solutions with varying concentrations were
138 prepared. For each solution, 2 mL was transferred into a test tube, followed by the addition of 500 μL of



139 Alcian blue solution for mixing. The mixture was then filtered through a polycarbonate filter membrane. The
140 subsequent steps for dissolving and measuring the membrane samples were conducted in accordance with
141 the procedures used for TEP.

142 **2.2.4 Pigments**

143 Water samples were quantitatively filtered using a Whatman glass fiber filter membrane with a pore size of
144 0.7 μm . The filtered membrane samples were stored in the dark at $-80\text{ }^{\circ}\text{C}$. Pigments were extracted by adding
145 3 mL of methanol at $-20\text{ }^{\circ}\text{C}$ for 2 hours, followed by ultrasonication in an ice water bath for 30 seconds. The
146 extract was then filtered through a syringe filter (4 mm, 0.45 μm PTFE, Whatman) to remove any debris. The
147 resulting extract was evaporated to dryness under a stream of nitrogen gas and subsequently reconstituted in
148 300 μL of a methanol-water mixture (19:1, v/v). Analysis of the samples was conducted within 4 hours.
149 Chromatographic analysis was performed using an Acquity UPLC® BEH C18 column (50 mm length, 1.7
150 μm particle size, 2.1 mm diameter) equipped with a PDA e λ detector and a fluorescence detector (UPLC,
151 Waters Corp., Milford, USA). Qualitative and quantitative analysis of pigments was conducted by comparing
152 the characteristic absorption wavelengths, peak areas, and peak times of pigment standards from the Danish
153 Institute of Water Environment, Denmark. The precision and detection limit of the instrument were 0.26
154 $\text{mg} \cdot \text{m}^{-3}$ and 2.2 $\text{mg} \cdot \text{m}^{-3}$, respectively (It should be noted that the method uses methanol as the solvent to
155 concentrate the sample, and its precision and detection limit may be more than 10 times higher than the
156 original sample). The pigment concentrations obtained using the CHEMTAX software allow for the
157 estimation of Chl *a* contributions from individual phytoplankton groups (Alderkamp et al., 2012; Mackey et
158 al., 1996). Specifically, fucoxanthin is the characteristic pigment associated with diatoms, 19'-
159 hexanoyloxyfucoxanthin with haptophytes (primarily *P. antarctica*), peridinin with dinoflagellates,
160 alloxanthin with cryptophytes and lutein with chlorophytes (Wright et al., 2010).

161 **2.3 Data processing**

162 **2.3.1 Multiple linear regression (MLR) fitting**

163 The TEP release by each phytoplankton group follows a power law function as described in Eq. (1) (Hong et
164 al., 1997; Passow, 2002b):



$$TEP = A(Chl\ a)^B \quad (1)$$

In this equation, A quantifies the initial TEP production potential of phytoplankton, which varies significantly depending on group composition and physiological status. Higher A values correspond to greater TEP release capacity during early growth phases. Previous studies have established that TEP production efficiency typically declines as bloom progress (Waite et al., 1995; Passow, 2002b). The coefficient B , consistently observed to be <1 , reflects a density-dependent inhibition effect on TEP production. The A and B coefficients of various phytoplankton groups generally exhibit significant variability, influenced by factors such as nutrient availability (Schartau et al., 2007), CO_2 concentration (Engel, 2002), light conditions, and the dynamics of microbial communities (Hong et al., 1997). Theoretical A and B values are generally higher than those observed in natural aquatic environments. However, obtaining representative phytoplankton groups from the Cosmonaut Sea has proven challenging. Current data only provide A and B coefficients for haptophytes, diatoms, and dinoflagellates under mesoscale and in situ bloom conditions (Table 2). Compared to the multi-algae environment, the results presented in Table 2 offer the most accurate available approximation of theoretical A and B values for major phytoplankton groups. Consequently, we utilized these values as the theoretical foundation for subsequent fitting analyses.

180

Table 2 The relationship between TEP and Chl a during the mesocosm blooms (1400liter) and in situ blooms:

$TEP = A(Chl\ a)^B$ in $\mu g\ Xeq\ L^{-1}$ and in $\mu g\ L^{-1}$

Groups (Species)	Sample site	A	B	Reference
Dinoflagellates	Mesocosm 95	163	0.56	Passow, 2002a
Haptophytes (<i>P. antarctica</i>)	Mesocosm 96	106	0.76	Passow, 2002a
Diatoms	Baltic Sea	282	0.33	Engel, 1998

183

Researches have established that biological processes are the primary driver of TEP production in marine systems (Passow, 2002b). However, field observations reveal that environmental factors can substantially alter TEP release dynamics across different phytoplankton taxa, resulting in substantial spatial and temporal variability in TEP content (Engel et al., 2017). To quantitatively assess taxon-specific TEP contributions under natural conditions, we propose an environmental correction factor (β), representing the ratio of TEP released by phytoplankton in the natural environment to the theoretical value. Thus, in situ TEP production



190 can be expressed as the theoretical value multiplied by β . The following prerequisites must be fulfilled for
191 the model to function effectively: First, TEP are predominantly produced through biological processes, and
192 the contribution of non-biological processes is negligible, which has been already confirmed in the results of
193 correlation analysis in Part 3.2. Second, there should be no significant alterations in the structure of the
194 phytoplankton community at the marine stations, ensuring that the dominant algal groups remain consistent.
195 Third, haptophytes, diatoms and dinoflagellates are the principal contributors to TEP, while contributions
196 from other algal groups are minimal. Environmental factors such as water temperature and light primarily
197 exert indirect influences on TEP production by affecting phytoplankton growth. Given the minimal spatial
198 variation in surface water temperature ($\Delta T < 2.3^\circ\text{C}$), uniform non-limiting nutrient conditions ($\text{N/P} \approx 16$),
199 and consistent PAR levels across stations, environmental parameters exerted negligible direct physiological
200 impacts on phytoplankton TEP production. Consistent with regional microbial biomass observations (Han et
201 al., 2022), surface waters in our study area exhibited characteristically low abundances of picoeukaryotes and
202 prokaryotic cells. Given the homogeneity of environmental forcing and minimal microbial interference in the
203 study area, phytoplankton community structure is identified as the primary direct driver of TEP production
204 in the Cosmonaut Sea surface waters during austral summer. Finally, we present the formula Eq. (2) for TEP
205 content derived from MLR analysis.

$$206 \quad TEP = \sum_i (\beta_i TEP_i) + \varepsilon \quad (2)$$

207 where β_i represents the correction factors for haptophytes (β_{Hapt}), diatoms (β_{Diat}), and dinoflagellates
208 (β_{Dino}), respectively. TEP_i denotes the theoretical concentration of TEP released by haptophytes, diatoms,
209 and dinoflagellates. ε represents the residual term, encompassing the total TEP contribution from other
210 phytoplankton groups beyond haptophytes, diatoms, and dinoflagellates, as well as the random variation that
211 the model does not account for.

212 The objective of MLR is to identify a set of correction factor (β) that minimizes the discrepancy between the
213 predicted TEP values generated by the model and the actual observed values. This is typically accomplished
214 by minimizing the sum of the squared residuals, a technique known as the least squares method. In this study,
215 the theoretical TEP content released by haptophytes, diatoms, and dinoflagellates (independent variables)
216 was calculated separately. Subsequently, a fitting procedure was conducted to correlate these theoretical



values with the actual TEP content (dependent variable) using Matlab software (R2019a), with the specific modeling and calculation processes detailed in Supporting Information. The fitting coefficients and other relevant results were subsequently reported based on the fitting outcomes.

2.3.2 Percentage of meltwater

In polar environments, the melting of sea ice can significantly impact marine ecosystems. This study evaluates the effect of sea ice melting on the structure of phytoplankton communities by calculating the percentage of meltwater (MW%) using Eq. (3) (Rivaró et al., 2014):

$$MW\% = \left(1 - \frac{S_o - 6}{S_d - 6}\right) \times 100 \quad (3)$$

Here, S_o represents the salinity of the surface water, while S_d denotes the salinity of the deep water at the same station unaffected by the dilution from melting ice (in this paper, $d=300$ m). It is also assumed that the average salinity of sea ice is 6 (Ackley et al., 1979).

2.3.3 Correlation analysis and visualization

This study employs IBM SPSS Statistics (Version 22, <https://www.ibm.com/analytics/spss-statistics-software>) for statistical analysis and uses Ocean Data View (Version 5.1.7, <http://odv.awi.de>) and Origin (OriginPro Version 2022, <https://www.originlab.com>) for data visualization.

3 Results

3.1 Surface hydrographic variability in the Cosmonaut Sea

The results for key parameters in the surface layer of the Cosmonaut Sea are summarized in Table 3, with their spatial distributions illustrated in Figure 2. The mean surface water temperature was -0.62 ± 0.58 °C, with lower values in coastal regions and higher values offshore. Notably, the western sector of Cape Ann exhibited warmer waters compared to the eastern sector. The average salinity was 33.76 ± 0.19 ‰, with elevated values observed east of Cape Ann. Generally, salinity was higher near the coast compared to offshore, except in the nearshore area west of Cape Ann, where no significant salinity increase was detected. The MW% exceeded 2 % at most stations (excluding C9-11), indicating a substantial influence of ice melt. PAR levels



241 were higher west of Cape Ann compared to eastern areas, though no distinct overall pattern was evident.
242 Nutrient distributions exhibited considerable variability: Silicate, phosphate and nitrate showed similar
243 spatial trends, with higher concentrations in coastal zone and lower values offshore. In contrast, nitrite
244 exhibited an inverse distribution, with lower concentrations near the coast and higher values offshore.
245 Ammonium levels were lower in waters west of Cape Ann compared to eastern regions.

246

247 **Table 3 The range and mean values of key parameters in the surface layer of the Cosmonaut Sea.**

Parameter	Range	Average	± SD, N
Temp [°C]	-1.83 — 0.42	-0.62	0.58, 29
Salinity [‰]	33.27 — 34.17	33.76	0.19, 29
Silicate [$\mu\text{mol L}^{-1}$]	18.75 — 62.64	31.14	9.47, 29
Phosphate [$\mu\text{mol L}^{-1}$]	0.91 — 2.23	1.29	0.30, 29
Nitrate [$\mu\text{mol L}^{-1}$]	13.85 — 44.21	21.42	6.53, 29
Nitrite [$\mu\text{mol L}^{-1}$]	0.09 — 0.60	0.24	0.12, 29
Ammonium [$\mu\text{mol L}^{-1}$]	0.13 — 1.10	0.41	0.25, 29
PAR [$\text{E m}^{-2} \text{d}^{-1}$]	22.15 — 44.50	33.36	6.77, 29
MW%	1.6 — 5.0	3.2	0.7, 27
TEP [$\mu\text{g Xeq L}^{-1}$]	2.07 — 38.99	16.58	10.19, 29
Haptophytes [$\mu\text{g L}^{-1}$]	ND* — 1.29	0.31	0.31, 27
Diatoms [$\mu\text{g L}^{-1}$]	0.01 — 0.60	0.17	0.13, 27
Dinoflagellates [$\mu\text{g L}^{-1}$]	ND — 0.32	0.08	0.08, 27
Chlorophytes [$\mu\text{g L}^{-1}$]	ND — 0.10	0.02	0.03, 27
Cryptophytes [$\mu\text{g L}^{-1}$]	ND — 0.24	0.07	0.01, 27
Chl α [$\mu\text{g L}^{-1}$]	0.01 — 1.72	0.66	0.50, 27

*ND (Not Detected), which can be calculated by 0.

248

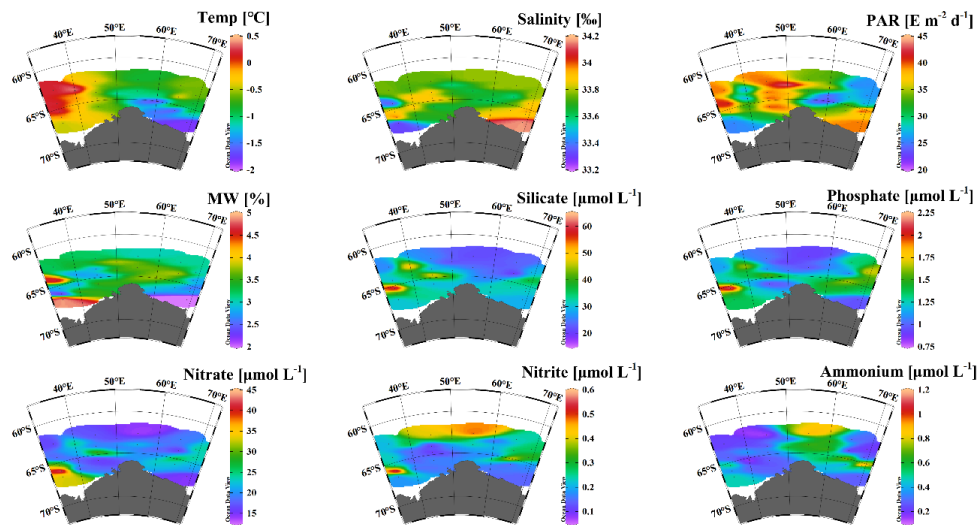


Figure 2 Distribution of hydrographic parameters in the surface layer of the Cosmonaut Sea

3.2 Distribution of TEP and Chl *a* in different phytoplankton groups

Figure 3 illustrates the spatial distributions of TEP and Chl *a*. The mean TEP concentration was $16.58 \pm 10.19 \mu\text{g Xeq L}^{-1}$, while the mean Chl *a* concentration was $0.66 \pm 0.50 \mu\text{g L}^{-1}$. Both parameters exhibited distinct spatial heterogeneity across Cape Ann waters, with elevated values in the WG region and significantly lower concentrations in eastern waters. The highest TEP concentration was recorded at station C3-07, while the peak Chl *a* was observed at station C4-03. Phytoplankton community composition analysis revealed that haptophytes dominated the phytoplankton community (mean concentration: $0.31 \pm 0.31 \mu\text{g L}^{-1}$), followed by diatoms and dinoflagellates. Cryptophytes and chlorophytes maintained consistently low abundances throughout the study area. As depicted in Figure 4, the relative abundance of the dominant phytoplankton groups followed the order: haptophytes > diatoms > dinoflagellates > other groups.

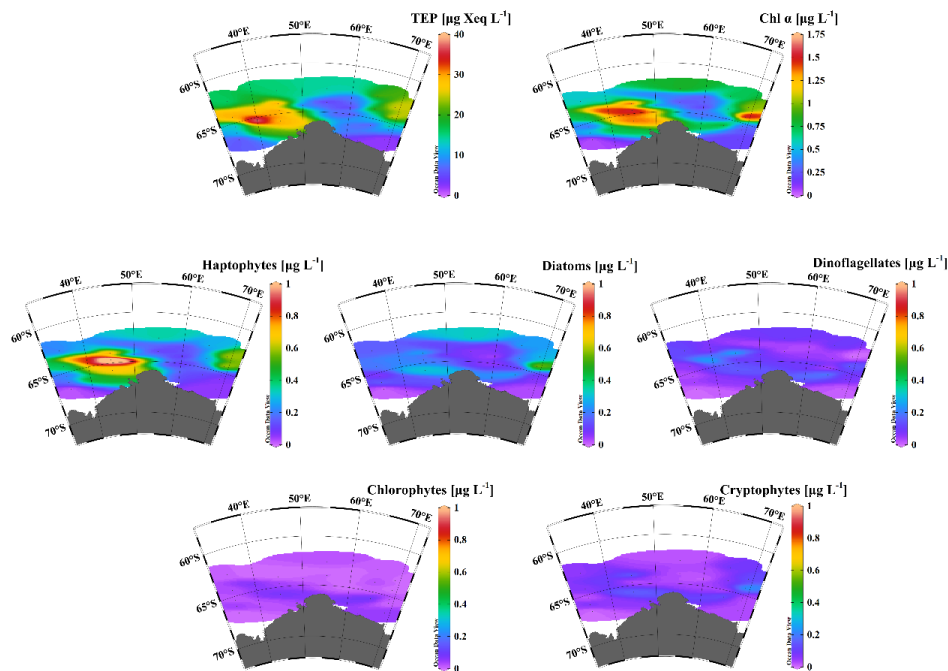


Figure 3 Distribution of TEP and phytoplankton biomass (Chl *a*) in the surface layer of the Cosmonaut Sea

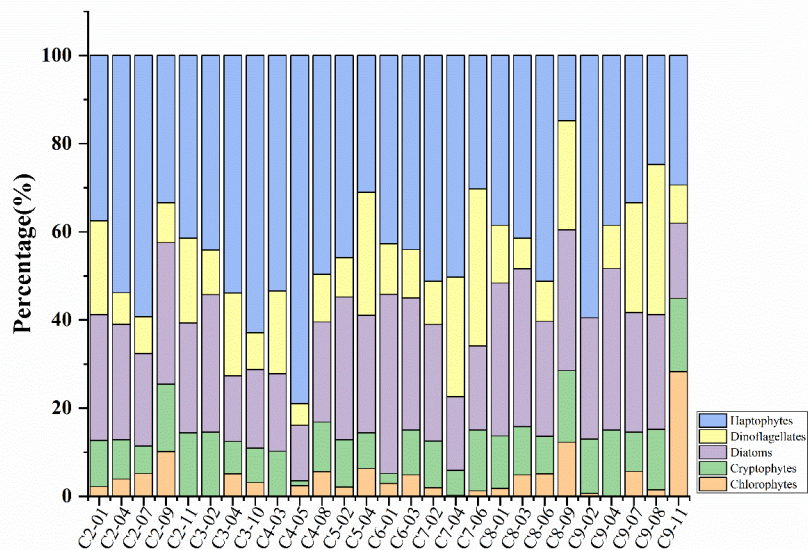


Figure 4 Phytoplankton population percentage in the surface layer of the Cosmonaut Sea



3.2 Analysis of relationships

The results of the correlation analysis (Figure 5) indicate that silicate levels are positively correlated with both phosphate and nitrate concentrations ($r = 0.81$, $p < 0.01$; $r = 0.62$, $p < 0.01$), while phosphate is also positively correlated with nitrate ($r = 0.66$, $p < 0.01$). Salinity exhibits a negative correlation with MW% ($r = -0.995$, $p < 0.01$). Furthermore, TEP shows positive correlations with all phytoplankton populations (haptophytes: $r = 0.86$, $p < 0.01$; diatoms: $r = 0.67$, $p < 0.01$; dinoflagellates: $r = 0.48$, $p < 0.05$; cryptophytes: $r = 0.60$, $p < 0.01$), except for chlorophytes. Additionally, TEP is negatively correlated with ammonium levels ($r = -0.50$, $p < 0.05$) and positively correlated with temperature ($r = 0.54$, $p < 0.01$).

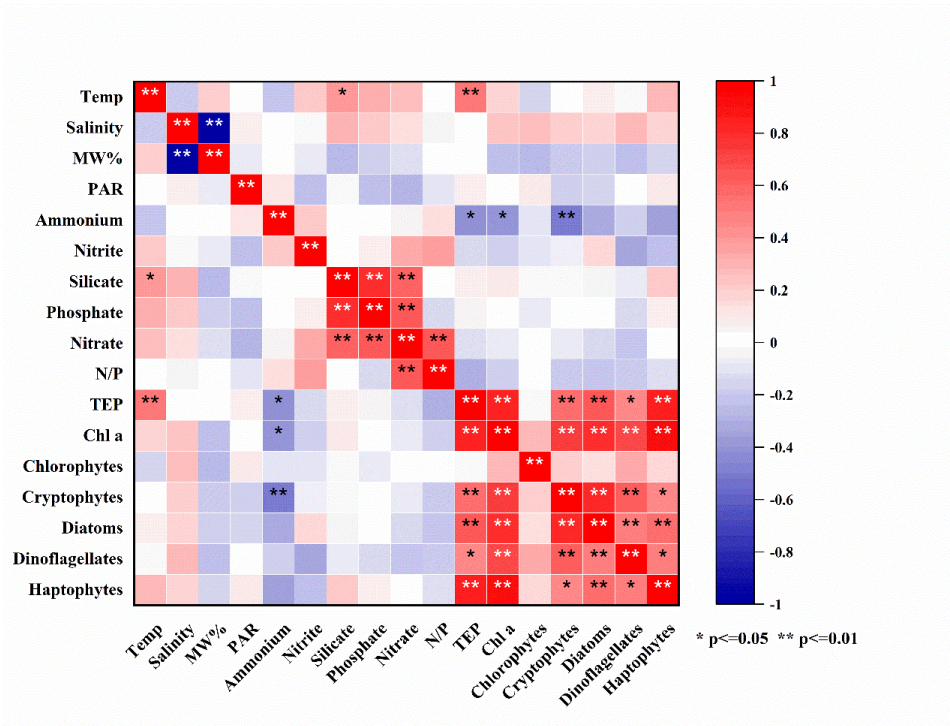


Figure 5 Heatmap of correlations among various parameters

3.3 Results of MLR fitting

Five stations (C7-04, C7-06, C8-09, C9-08, and C9-11) exhibited anomalous phytoplankton community compositions that significantly deviated from both other stations and our initial ecological assumptions (detailed in Supporting Information). Consequently, these outlier stations were excluded from subsequent



model fitting analyses. The regression results are summarized in Table 4. The initial MLR model yielded a non-significant intercept (ε) of -1.14 ($p = 0.77$), with correction coefficients of $\beta_{Hapt} = 0.189$ ($p < 0.01$), $\beta_{Diat} = 0.061$ ($p > 0.05$), and $\beta_{Dino} = 0.032$ ($p > 0.05$). While the model explained 83.1% of the variance in TEP production ($R^2 = 0.83$), the non-significant coefficients for β_{Diat} and β_{Dino} , along with the marginal significance of the intercept term, indicated potential for model refinement. Through stepwise model optimization, we constrained ε to zero and excluded β_{Dino} . The final optimized model demonstrated improved statistical performance, with significant β_{Hapt} (0.201, $p < 0.01$) and β_{Diat} (0.058, $p < 0.01$), with maintaining high explanatory power ($R^2 = 0.82$). The final results robustly quantify the differential contributions of phytoplankton groups to TEP production in Cosmonaut Sea surface waters, establishing haptophytes as primary contributors, followed by diatoms, while dinoflagellate showed no statistically significant contribution.

291

292 **Table 4 Results of MLR fitting**

Fitting result	Initial fitting			Final fitting		
	Value	SE	p	Value	SE	p
β_{Hapt}	0.189	0.041	0.0002	0.201	0.034	0.00001
β_{Diat}	0.061	0.032	0.07	0.058	0.012	0.0001
β_{Dino}	0.032	0.055	0.57	/	/	/
ε	-1.143	3.792	0.77	/	/	/
R ²	0.83			0.82		
Note: SE represents the standard error of the statistic; p < 0.05 indicates statistically significant, while p > 0.05 indicates non-significant; R ² denotes the coefficient of determination, with higher values indicating greater explanatory power of the model						

293 **4 Discussion**

294 **4.1 The effect of phytoplankton on the distribution of TEP**

As shown in Figure 3, both TEP and Chl *a* show significant enrichment in the WG region and at hydrographic frontal zones marking water mass convergence. A strong positive correlation was observed between TEP and Chl *a* ($r = 0.89$, $p < 0.01$), indicating that phytoplankton are the predominant source of TEP (Passow, 2002a; Passow, 2002b). The WG region is characterized by upwelling and hosts a persistent polynya known as the



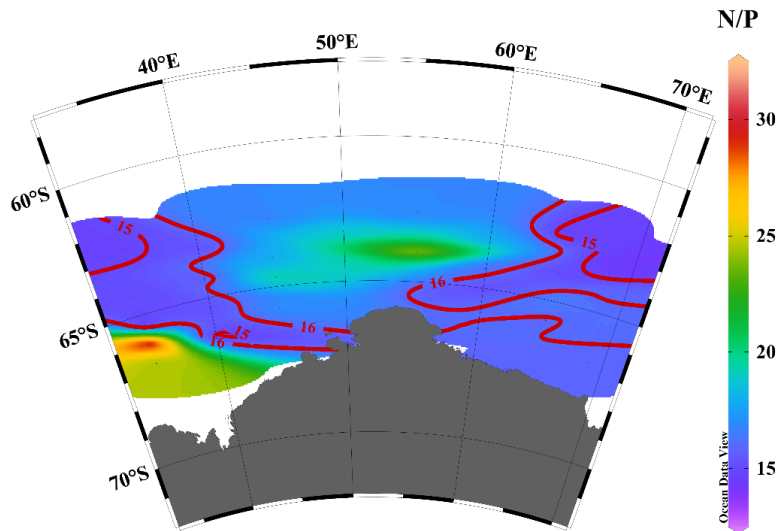
299 sensible heat polynya (Williams et al., 2010; Geddes and Moore, 2007). This polynya enhances vertical
300 nutrient flux from subsurface layers (Zhan et al., 2023) and contributes to a reduction in mixed layer depth
301 (Xue et al., 2023). The shallower mixed layer facilitates light availability for phytoplankton in the photic
302 zone (Le Grix et al., 2021; Noh et al., 2022), thereby stimulating phytoplankton blooms and increasing their
303 abundance in the WG region. The ACC is primarily comprised of Circumpolar Deep Water (CDW), which
304 originates in the North Atlantic and undergoes eastward transport around Antarctica (Pakhomov, 2000). CDW
305 is characterized by elevated heat content and enhanced nutrient concentrations (Martinson, 2012; Williams
306 et al., 2010). Moreover, the frontal zone between the ACC and ASC frequently exhibits divergent upwelling
307 features (Park et al., 1998; Williams et al., 2010). This upwelling process increases nutrient availability within
308 the convergence zone, stimulating phytoplankton proliferation. The subsequent phytoplankton blooms
309 enhance TEP release, leading to elevated TEP concentrations in these regions.

310 Previous studies have demonstrated that extracellular polymer production is regulated by nitrogen and
311 phosphorus availability (Guerrini et al., 2000; Magaletti et al., 2004; Li et al., 2020). Under low nitrogen
312 conditions, nutrient depletion in algal cells can induce physiological stress, leading to increased secretion of
313 extracellular substances (Granum et al., 2002; Yang et al., 2010; Staats et al., 2000; Barcelos et al., 2020). As
314 shown in Table 3, nitrate concentrations exceeded $10 \mu\text{mol L}^{-1}$, while phosphate concentrations were above
315 $0.3 \mu\text{mol L}^{-1}$, indicating no nutrient limitation (Moore et al., 2013). The Redfield ratio (C:N:P = 106:16:1)
316 serves as a fundamental reference for evaluating nutrient limitation in marine systems (Redfield, 1958;
317 Tanioka et al., 2022). To evaluate potential nutrient limitations, we calculated the nitrogen-to-phosphorus
318 (N/P) ratio from available nutrient data (Figure 6). The results reveal that most surface waters in the
319 Cosmonaut Sea are not nitrogen-limited, with N/P ratios primarily ranging between 15–16. Additionally,
320 correlation analysis (Figure 4) revealed no significant relationship between N/P ratios and TEP or
321 phytoplankton biomass, suggesting that nutrient availability does not exert a primary limiting effect on
322 phytoplankton growth in this region.

323 Notably, ammonium (NH_4^+) shows a negative correlation with TEP, cryptophytes, diatoms, and haptophytes,
324 indicating that under nutrient-replete conditions, ammonium assimilation may stimulate the growth of these
325 phytoplankton groups, thereby enhancing TEP production. This pattern likely reflects the preferential uptake



326 of ammonium over nitrate by phytoplankton (Karasiewicz et al., 2018; Xu et al., 2022). In particular,
327 haptophytes exhibit greater ammonium uptake efficiency compared to diatoms (Tungaraza et al., 2003),
328 which explains their elevated abundance in the study area (Figure 4). Additionally, MW% data from the
329 region (Figure 2) reveal that the surface layer of the Cosmonaut Sea is affected by meltwater input (MW% >
330 2%), which may enhance water column stratification and potentially favor phytoplankton growth (Massolo
331 et al., 2009; Rivaro et al., 2014). However, the absence of significant correlation between MW% and
332 phytoplankton abundance suggests that meltwater does not act as a primary limiting factor for phytoplankton
333 growth. In summary, nutrient availability in both the WG region and the water mass convergence zone
334 remains non-limiting, while favorable light conditions further promote phytoplankton proliferation and the
335 subsequent release of substantial TEP quantities.



336
337 **Figure 6 The ratio of N/P in the surface layer of the Cosmonaut Sea**
338 **($N/P = (\text{Ammonium} + \text{Nitrite} + \text{Nitrate}) / \text{Phosphate}$. The red solid line ($N/P = 16$) denotes the nutrient limitation**
339 **threshold, and $N/P < 16$ indicates nitrogen limitation)**

340 **4.2 The effects of temperature, ammonium and polysaccharide components on the correction**
341 **coefficient**

342 The regression fitting yielded R^2 values of 0.83 and 0.82, respectively, indicating robust explanatory power
343 of the models. These results demonstrate that the selected independent variables significantly predict the



344 dependent variable, supporting our hypothesis regarding the linear relationship between TEP concentration
345 and theoretical TEP production by individual phytoplankton groups. Statistical analysis revealed significant
346 correction coefficients for haptophytes (β_{Hapt}) and diatoms (β_{Diat}), with p-values < 0.05 , confirming their
347 substantial contribution to TEP content. In contrast, non-significant p-values ($p > 0.05$) were obtained for
348 both dinoflagellates (β_{Dino}) and the intercept term (ϵ), suggesting their negligible effects on the model. The
349 final simplified linear regression model Eq. (3) can be expressed as:

$$350 \quad TEP = 0.201TEP_{Hapt} + 0.058TEP_{Diat} \quad (3)$$

351 The regression analysis revealed that β_{Diat} was lower than β_{Hapt} , indicating greater deviation from
352 theoretical TEP values for diatoms. This suggests that diatom-associated TEP production is more sensitive to
353 environmental variability compared to haptophytes. Although numerous environmental factors including
354 light intensity, photoperiod, and spectral quality are known to regulate algal extracellular polysaccharide
355 secretion in a species-specific manner (Price et al., 1998; Otero and Vincenzini, 2003; You and Barnett, 2004),
356 our correlation analyses showed no significant relationship between PAR and either TEP or phytoplankton
357 biomass. This finding suggests that light conditions do not constitute a primary controlling factor in our study
358 region.

359 Microalgal extracellular polymer synthesis is regulated by temperature, as the enzymatic processes involved
360 often possess different thermal optima compared to those controlling microbial growth (Barcelos et al., 2020).
361 Polar diatoms adapt to subzero temperatures (-4°C) by upregulating carbohydrate metabolism enzymes,
362 thereby increasing extracellular polymer production to maintain cellular protection (Aslam et al., 2018).
363 However, at elevated temperatures, these enzymatic activities may become less efficient, potentially reducing
364 diatom contributions to TEP formation. In our study region, where surface water temperatures consistently
365 remain above -4°C , warming conditions could reduce the efficiency of diatom-mediated TEP synthesis. In
366 contrast, haptophytes, exhibiting greater thermal adaptation to warmer waters (Van Rijssel et al., 2000; Cheng
367 et al., 2023), display less temperature-dependent variation in TEP production, explaining their higher
368 correction coefficient relative to diatoms. It should be noted that although water temperature exhibited limited
369 spatial variability across the study area ($\Delta T < 2.3^{\circ}\text{C}$), it served as a uniform background driver that
370 systematically modulated the competitive balance between diatoms and haptophytes. The higher β



371 coefficient for haptophytes (0.201 vs. 0.058 for diatoms) suggests that even within this narrow thermal range,
372 the ambient temperature near 0°C favored haptophytes in TEP production efficiency. This mechanism
373 operates homogeneously across the region rather than generating spatial contrasts. The apparent positive
374 correlation between temperature and TEP ($r = 0.54$, $p < 0.01$) likely stems from co-variation with biological
375 processes. When phytoplankton biomass is accounted for, the direct effect of the narrow temperature range
376 ($< 2.3^{\circ}\text{C}$) on TEP is likely negligible, as confirmed by the dominance of community structure effects in the
377 MLR model.

378 Nutrient availability significantly regulates phytoplankton extracellular polymer production. As established
379 earlier, the surface waters of the Cosmonaut Sea exhibit no-limiting nutrient conditions. Of particular
380 ecological relevance, haptophytes demonstrate enhanced ammonium assimilation efficiency compared to
381 diatoms, a physiological advantage contributing to their numerical dominance. The substantial proliferation
382 of haptophytes can induce cyst formation (Hamm, 2000), a process with dual ecological implications: these
383 cysts may provide microhabitats for other algal species (Rousseau et al., 1994; Hamm and Rousseau, 2003),
384 yet simultaneously harbor symbiotic *Vibrio* bacteria (Cho et al., 2017). These associated *Vibrio* species
385 possess laminarinase-producing capabilities (Alderkamp et al., 2007b), potentially compromising
386 polysaccharide synthesis through laminarin degradation. Furthermore, *Vibrio* bacteria exhibit significant
387 algicidal activity (Dungca-Santos et al., 2019) and demonstrate competitive inhibition against diatoms and
388 other phytoplankton groups (Liu et al., 2008). Ammonium concentration appears to be a critical regulator of
389 *Vibrio*-phytoplankton population dynamics (Xu et al., 2022). Consequently, elevated ammonium levels may
390 stimulate *Vibrio* proliferation, leading to suppressed diatom metabolic activity. This intricate trophic
391 interaction network likely explains the observed differential regression coefficients between diatoms (lower)
392 and haptophytes (higher).

393 The carbohydrate pool of Southern Ocean diatoms is predominantly composed of glucose, which constitutes
394 a major fraction of total carbohydrates (Alderkamp et al., 2007a; van Oijen et al., 2003). As a simple
395 monosaccharide, glucose lacks sulfate ester groups (R-OSO_3^-) (Zhou et al., 1998). In contrast, haptophyte-
396 derived polysaccharides (e.g., fucoidan) typically contain elevated concentrations of these anionic functional
397 groups, which facilitate ionic bond formation (Smith et al., 1995; Van Boekel et al., 1992). This structural



398 difference confers greater resistance to microbial degradation on haptophyte polysaccharides compared to
399 diatom-derived compounds. Consequently, diatom-associated TEP exhibits reduced persistence in the marine
400 environment, explaining the observed lower correction coefficient for diatoms relative to haptophytes in our
401 analysis.

402 **4.3 The contribution of different phytoplankton groups to TEP**

403 Laboratory-controlled experiments demonstrate a positive correlation between group-specific TEP
404 production and Chl *a* concentrations. As illustrated in Figure 7(a), diatoms consistently exhibit higher TEP
405 release rates than haptophytes, corroborating previous findings that diatoms contribute more substantially to
406 TEP production per unit biomass than haptophytes (Passow, 2002a; Passow, 2002b). However, our field
407 observations reveal a contrasting pattern when correction coefficients are applied: the TEP production
408 dynamics between these phytoplankton groups show distinct biomass-dependent trends. At equivalent
409 biomass levels (represented by Chl *a* below 0.5 $\mu\text{g L}^{-1}$), diatoms maintain their characteristic elevated TEP
410 production compared to haptophytes. This relationship undergoes a marked reversal at higher biomass
411 concentrations (Chl *a* > 0.5 $\mu\text{g L}^{-1}$), where haptophytes demonstrating significantly greater TEP release than
412 diatoms, as shown in Figure 7(b).

413 To quantitatively assess these contributions, we derived corrected TEP values (designated TEP_d-Hapt and
414 TEP_d-Diat) by applying group-specific correction coefficients to theoretical TEP contents. Comparative
415 analysis of these corrected values with measured TEP concentrations (Figure 8) reveals a clear ecological
416 transition: in haptophyte-dominated waters, diatoms contribute more substantially to TEP pools at low
417 phytoplankton biomass (Chl *a* < 0.5 $\mu\text{g L}^{-1}$), while haptophytes emerge as the dominant TEP producers at
418 higher biomass levels.

419 Existing literature has established both diatoms (Mari and Burd, 1998; Fukao et al., 2010) and haptophytes
420 (Hong et al., 1997) as important sources of TEP, with diatoms generally considered the predominant
421 contributors (Alldredge et al., 1993; Ramaiah et al., 2001; Azetsu-Scott and Passow, 2004). However, our
422 findings demonstrate that phytoplankton contributions to TEP production exhibit strong dependence on
423 interspecific variations in Chl *a* content among dominant groups. This biomass-dependent variation in TEP



424 production may be attributed to competitive interactions between phytoplankton groups, consistent with
425 previous ecological observations (Liu et al., 2008).

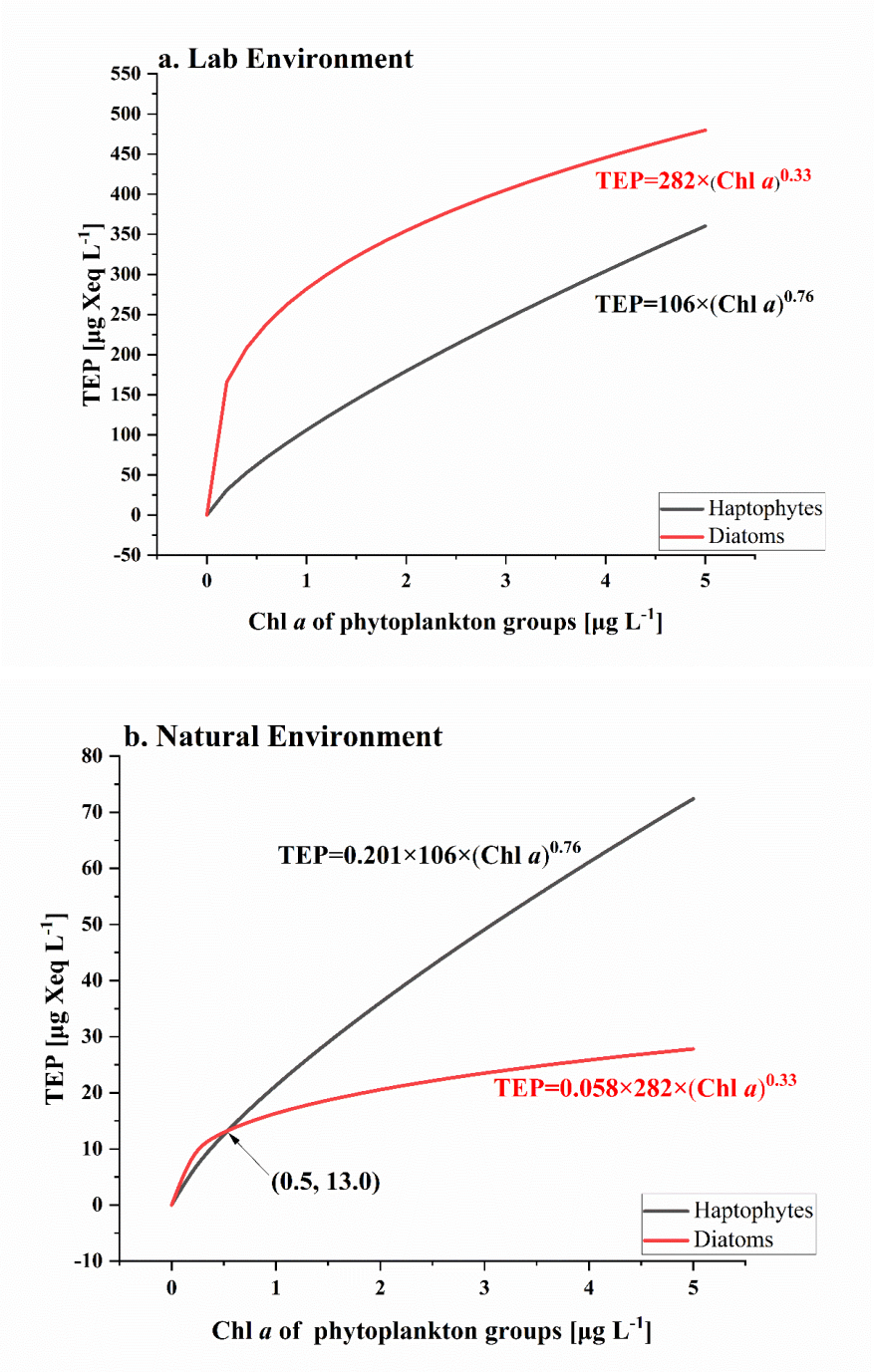


Figure 7 The release of TEP by haptophytes and diatoms at varying concentrations of Chl *a* (a. laboratory environment, with the empirical formula is derived from Passow (2002b) ; b. natural environment)

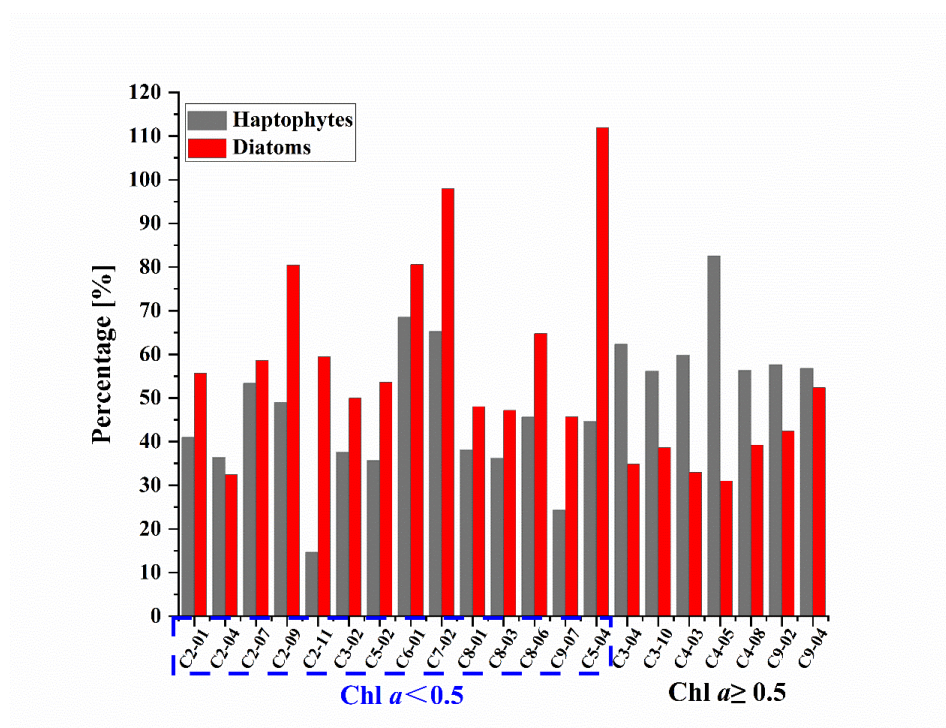


Figure 8 Differences in the contribution of haptophytes and diatoms to TEP production in the surface layer of the Cosmonaut Sea

Biomass-corrected TEP concentrations derived from haptophytes and diatoms are presented in Figure 9(a) and 9(b), respectively. In the surface waters of the Cosmonaut Sea, haptophyte-derived TEP concentrations ranged from 0.9 to 28.0 $\mu\text{g Xeq L}^{-1}$, while diatom-derived TEP ranged from 2.8-11.4 $\mu\text{g Xeq L}^{-1}$. These observed TEP concentration ranges align well with established empirical relationships describing phytoplankton abundance and TEP production capacity (Berman and Viner-Mozzini, 2001; Passow, 2002a; Passow, 2002b). When integrated with phytoplankton distribution patterns shown in Figure 3, these results suggest that both haptophytes and diatoms likely experienced bloom conditions in the WG region and water mass convergence zones, leading to enhanced TEP production. Notably, the spatial distribution of haptophyte-derived TEP closely corresponds to the measured bulk TEP concentrations (Figure 3), with the highest values concentrated in the WG region and frontal convergence zones. In contrast, diatom-derived TEP displayed a more homogeneous spatial distribution, with peak concentrations occurring in areas distinct



444 from haptophyte-dominated regions. This spatial differentiation may reflect competitive interactions between
445 phytoplankton groups (Liu et al., 2008).

446 The relative contributions of different phytoplankton groups to TEP production are presented in Figure 9(c)
447 and 9(d). Assuming TEP originates predominantly from haptophytes and diatoms, their cumulative
448 contributions should approximate 100% of total TEP. Our results confirm this theoretical expectation in the
449 WG region and water mass convergence zones, where the cumulative contributions of these two groups
450 approach 100%, establishing their predominance in TEP production in these areas. A notable exception occurs
451 at station C6-03, where the calculated contribution exceeds 100%. This discrepancy likely reflects the
452 exceptionally low measured TEP concentration ($3.55 \mu\text{g Xeq L}^{-1}$), which approaches both the methodological
453 detection limit ($2.45 \mu\text{g Xeq L}^{-1}$ for colorimetric determination) and the measurement uncertainty range (\pm
454 $2.27 \mu\text{g Xeq L}^{-1}$). Excluding this outlier, our data show that haptophytes contribute 14.6 – 82.5% (mean: $48.6 \pm 15.4\%$) of total TEP, while diatoms account for 31.0 – 112.0% (mean: $55.1 \pm 21.2\%$). The comparable
456 magnitude of contributions from both phytoplankton groups underscores the previously underestimated
457 importance of haptophytes in TEP production. These findings highlight the crucial role of haptophytes in
458 Southern Ocean carbon cycling processes, prompting a necessary reassessment of their ecological
459 significance in the marine ecosystem.

460

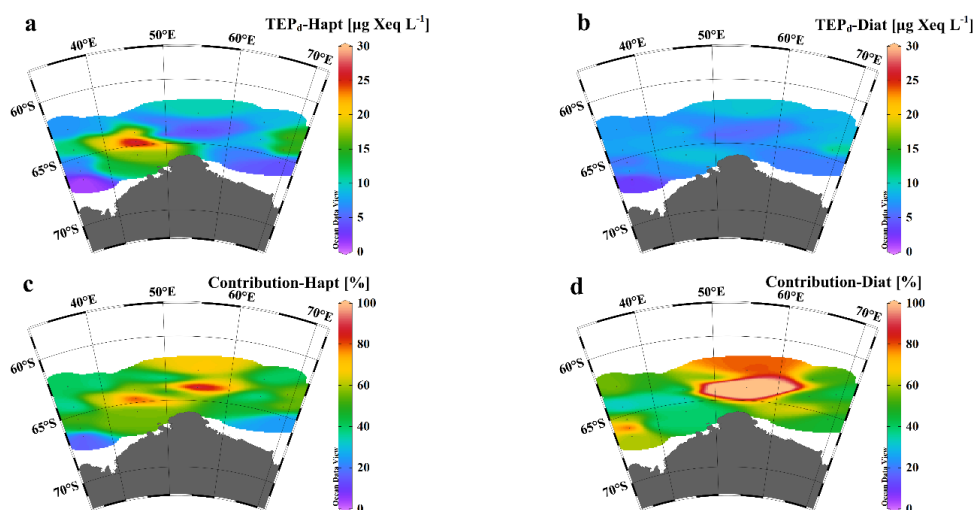


Figure 9 Contribution of haptophytes and diatoms to TEP (a and b represent the biomass-corrected TEP concentrations derived from haptophytes and diatoms, respectively; c and d depict the relative contributions of haptophytes and diatoms to TEP, respectively.)

5 Conclusion

This study analyzed surface water samples from the Cosmonaut Sea, measuring TEP, Chl *a* and key environmental parameters to characterize TEP distribution. The observed spatial heterogeneity in TEP distribution was predominantly driven by phytoplankton community structure. Our MLR model quantified group-specific TEP contributions through environmentally adjusted correction factors (β), revealing significantly higher β for haptophytes (0.201) than diatoms (0.058). This discrepancy reflects group-specific physiological responses to ambient conditions, where temperature, ammonium, and polysaccharide composition indirectly regulate TEP production efficiency via community dynamics. Quantitative analysis demonstrated that haptophytes contributed 14.6 – 82.5% (mean $48.6 \pm 15.4\%$) of total TEP, while diatoms accounted for 31.0 – 112.0% (mean $55.1 \pm 21.2\%$). Critically, we establish a new paradigm that diatoms dominate TEP production when *P. antarctica* Chl *a* $< 0.5 \mu\text{g L}^{-1}$, while haptophytes emerge as the predominant TEP producers at elevated biomass. This biomass-dependent inversion, undocumented in laboratory studies, highlights the necessity of in situ community-level assessments.



478 These results recalibrate our understanding of polar carbon cycling by revealing the pivotal role of *P.*
479 *antarctica* in Southern Ocean biogeochemistry. While this study provides critical insights, several limitations
480 should be acknowledged: First, the exclusive focus on surface waters during austral summer precludes
481 assessment of seasonal variability or vertical flux dynamics. Second, while our MLR model effectively
482 captured phytoplankton-driven TEP production, it inherently simplified the potential contributions of abiotic
483 processes and bacterial remineralization.

484 To address these limitations and advance the field, we propose four key research priorities:

485 (i) Comprehensive multi-seasonal sampling across water column depths to characterize full phenological
486 patterns of TEP production and export;

487 (ii) Controlled mechanistic experiments to quantify how environmental parameters (temperature, nutrients,
488 light) modulate taxon-specific β factors;

489 (iii) Application of metatranscriptomic approaches to identify genetic markers of TEP synthesis and their
490 expression patterns in natural phytoplankton assemblages;

491 (iv) Systematic quantification of bacterial TEP degradation rates in polar surface waters to constrain this
492 potentially important sink term.

493 **Data availability statement**

494 All data generated or analyzed during this study are included in this published article and its supplementary
495 materials. The supplement related to this article is available online at
496 <https://doi.org/10.5281/zenodo.16020210>.

497 **Author contribution**

498 SYX is responsible for research design, data analysis, and manuscript writing. JH contributed to research
499 design, data verification, and manuscript revision. JZ, DL, HFZ, XFY, CZ, PSY, CFZ, and KYT participated
500 in data provision, sample collection, and manuscript editing. GJF, JMP, and MC provided technical and
501 financial support.

502 **Competing interests**



503 The contact author has declared that none of the authors has any competing interests.

504 Acknowledgements

505 This research was funded by the National Natural Science Foundation of China (No. 42276255, 41976227
506 and 42306262) and the project “Impact and Response of Antarctic Seas to Climate Change, IRASCC 2020-
507 2022” (Nos. 01-01-02A and B, 02-02-03, 02-02-05, and 02-01-01).

508 Reference

- 509 Ackley S. F., Buck K. R. and Taguchi S.: Standing crop of algae in the sea ice of the Weddell Sea region,
510 Deep-Sea Research Part A. Oceanographic Research Papers, 26, 269-281, doi:10.1016/0198-
511 0149(79)90024-4, 1979.
- 512 Alderkamp A.-C., Buma A. G. and van Rijssel M.: The carbohydrates of Phaeocystis and their degradation
513 in the microbial food web, Biogeochemistry, 83, 99-118, doi:10.1007/978-1-4020-6214-8_9, 2007a.
- 514 Alderkamp A.-C., Mills M. M., van Dijken G. L., et al. Buma A. G.: Iron from melting glaciers fuels
515 phytoplankton blooms in the Amundsen Sea (Southern Ocean): Phytoplankton characteristics and
516 productivity, Deep-Sea Research Part II: Topical Studies in Oceanography, 71, 32-48,
517 doi:10.1016/j.dsr2.2012.03.005, 2012.
- 518 Alderkamp A.-C., Van Rijssel M. and Bolhuis H.: Characterization of marine bacteria and the activity of their
519 enzyme systems involved in degradation of the algal storage glucan laminarin, FEMS Microbiology
520 Ecology, 59, 108-117, doi:10.1111/j.1574-6941.2006.00219.x, 2007b.
- 521 Alldredge A. L., Passow U. and Logan B. E.: The abundance and significance of a class of large, transparent
522 organic particles in the ocean, Deep-Sea Research Part I-Oceanographic Research Papers, 40, 1131-
523 1140, doi:10.1016/0967-0637(93)90129-q, 1993.
- 524 Aluwihare L. I. and Repeta D. J.: A comparison of the chemical characteristics of oceanic DOM and
525 extracellular DOM produced by marine algae, Marine Ecology Progress Series, 186, 105-117,
526 doi:10.3354/meps186105, 1999.
- 527 Arrigo K. R., van Dijken G. and Long M.: Coastal Southern Ocean: A strong anthropogenic CO₂ sink,
528 Geophysical Research Letters, 35, doi:10.1029/2008gl035624, 2008.
- 529 Arrigo K. R., van Dijken G. L. and Strong A. L.: Environmental controls of marine productivity hot spots
530 around a ntarctica, Journal of Geophysical Research: Oceans, 120, 5545-5565,
531 doi:10.1002/2015jc010888, 2015.
- 532 Arteaga L., Haentjens N., Boss E., Johnson K. S. and Sarmiento J. L.: Assessment of export efficiency
533 equations in the Southern Ocean applied to satellite-based net primary production, Journal of
534 Geophysical Research-Oceans, 123, 2945-2964, doi:10.1002/2018jc013787, 2018.
- 535 Aslam S. N., Strauss J., Thomas D. N., Mock T. and Underwood G. J.: Identifying metabolic pathways for
536 production of extracellular polymeric substances by the diatom *Fragilariopsis cylindrus* inhabiting
537 sea ice, The ISME journal, 12, 1237-1251, doi:10.1038/s41396-017-0039-z, 2018.



- 538 Azetsu-Scott K. and Passow U.: Ascending marine particles: Significance of transparent exopolymer particles
539 (TEP) in the upper ocean, *Limnology and Oceanography*, 49, 741-748,
540 doi:10.4319/lo.2004.49.3.0741, 2004.
- 541 Barcelos M. C., Vespermann K. A., Pelissari F. M. and Molina G.: Current status of biotechnological
542 production and applications of microbial exopolysaccharides, *Critical Reviews in Food Science and*
543 *Nutrition*, 60, 1475-1495, doi:10.1080/10408398.2019.1575791, 2020.
- 544 Berman T. and Viner-Mozzini Y.: Abundance and characteristics of polysaccharide and proteinaceous
545 particles in Lake Kinneret, *Aquatic Microbial Ecology*, 24, 255-264, doi:10.3354/ame024255, 2001.
- 546 Biddanda B. and Benner R.: Carbon, nitrogen, and carbohydrate fluxes during the production of particulate
547 and dissolved organic matter by marine phytoplankton, *Limnology and Oceanography*, 42, 506-518,
548 doi:10.4319/lo.1997.42.3.0506, 1997.
- 549 Cheng H.-M., Zhang S.-F., Ning X.-L., et al. Smith Jr W. O.: Elucidating colony bloom formation mechanism
550 of a harmful alga *Phaeocystis globosa* (Prymnesiophyceae) using metaproteomics, *Science of the*
551 *Total Environment*, 869, 161846, doi:10.1016/j.scitotenv.2023.161846, 2023.
- 552 Cho K., Wencheng L., Takeshita S., Seo J.-K., Chung Y.-H., Kim D. and Oda T.: Evidence for the presence
553 of cell-surface-bound and intracellular bactericidal toxins in the dinoflagellate *Heterocapsa*
554 *circularisquama*, *Aquatic Toxicology*, 189, 209-215, doi:10.1016/j.aquatox.2017.06.016, 2017.
- 555 DeVore C. and Kaukis N.: Linear regression analysis, *STAT*, 3013, 15, doi:10.5455/jmood.20130624120840,
556 2003.
- 557 Dungca-Santos J. C. R., Caspe F. J. O., Tablizo F. A., Purganan D. J. E., Azanza R. V. and Onda D. F. L.:
558 Algicidal potential of cultivable bacteria from pelagic waters against the toxic dinoflagellate
559 *Pyrodinium bahamense* (Dinophyceae), *Journal of Applied Phycology*, 31, 3721-3735,
560 doi:10.1007/s10811-019-01839-0, 2019.
- 561 Engel, Anja. *Bildung, Zusammensetzung und Sinkgeschwindigkeiten mariner Aggregate*. Diss. Institut für
562 *Meereskunde*, 1998.
- 563 Engel A.: Direct relationship between CO₂ uptake and transparent exopolymer particles production in natural
564 phytoplankton, *Journal of Plankton Research*, 24, 49-53, doi:10.1093/plankt/24.1.49, 2002.
- 565 Engel A.: Distribution of transparent exopolymer particles (TEP) in the northeast Atlantic Ocean and their
566 potential significance for aggregation processes, *Deep Sea Research Part I: Oceanographic Research*
567 *Papers*, 51, 83-92, doi:10.1016/j.dsr.2003.09.001, 2004.
- 568 Engel A., Goldthwait S., Passow U. and Alldredge A.: Temporal decoupling of carbon and nitrogen dynamics
569 in a mesocosm diatom bloom, *Limnology and Oceanography*, 47, 753-761,
570 doi:10.4319/lo.2002.47.3.0753, 2002.
- 571 Engel A., Piontek J., Metfies K., Endres S., Sprong P., Peeken I., Gaebler-Schwarz S. and Noethig E.-M.:
572 Inter-annual variability of transparent exopolymer particles in the Arctic Ocean reveals high
573 sensitivity to ecosystem changes, *Scientific Reports*, 7, doi:10.1038/s41598-017-04106-9, 2017.
- 574 Engel A. and Schartau M.: Influence of transparent exopolymer particles (TEP) on sinking velocity of
575 *Nitzschia closterium* aggregates, *Marine Ecology Progress Series*, 69-76, doi:10.3354/meps182069,
576 1999.
- 577 Fukao T., Kimoto K. and Kotani Y.: Production of transparent exopolymer particles by four diatom species,
578 *Fisheries Science*, 76, 755-760, doi:10.1007/s12562-010-0265-z, 2010.



- 579 Ge Z., Li Q. P., Yang W., Liu X. and Wu Z.: Transparent exopolymer particle dynamics along a shelf-to-sea
580 gradient and impacts on the regional carbon cycle, *Science of the Total Environment*, 808,
581 doi:10.1016/j.scitotenv.2021.152117, 2022.
- 582 Geddes J. A. and Moore G.: A climatology of sea ice embayments in the Cosmonaut Sea, Antarctica,
583 *Geophysical Research Letters*, 34, doi:10.1029/2006gl027910, 2007.
- 584 Granum E., Kirkvold S. and Mykkestad S. M.: Cellular and extracellular production of carbohydrates and
585 amino acids by the marine diatom *Skeletonema costatum*: diel variations and effects of N depletion,
586 *Marine Ecology Progress Series*, 242, 83-94, doi:10.3354/meps242083, 2002.
- 587 Guerrini F., Cangini M., Boni L., Trost P. and Pistocchi R.: Metabolic responses of the diatom *Achnanthes*
588 *brevipes* (Bacillariophyceae) to nutrient limitation, *Journal of Phycology*, 36, 882-890,
589 doi:10.1046/j.1529-8817.2000.99070.x, 2000.
- 590 Guo K. L., Chen J., Yuan J., Wang X. D., Xu S. S., Hou S. W. and Wang Y.: Effects of temperature on
591 transparent exopolymer particle production and organic carbon allocation of four marine
592 phytoplankton species, *Biology-Basel*, 11, 15, doi:10.3390/biology11071056, 2022.
- 593 Hamm C.: Architecture, ecology and biogeochemistry of *Phaeocystis* colonies, *Journal of Sea Research*, 43,
594 307-315, doi:10.1016/s1385-1101(00)00014-9, 2000.
- 595 Hamm C. E. and Rousseau V.: Composition, assimilation and degradation of *Phaeocystis globosa*-derived
596 fatty acids in the North Sea, *Journal of Sea Research*, 50, 271-283, doi:10.1016/s1385-
597 1101(03)00044-3, 2003.
- 598 Han M., Cao S., Luo G., et al. Zhang W.: Distributions of virio- and picoplankton and their relationships with
599 ice-melting and upwelling in the Indian Ocean sector of East Antarctica, *Deep Sea Research Part II:*
600 *Topical Studies in Oceanography*, 197, 105044, 2022.
- 601 Hong Y., Smith W. O. and White A. M.: Studies on transparent exopolymer particles (TEP) produced in the
602 Ross Sea (Antarctica) and by *Phaeocystis antarctica* (Prymnesiophyceae), *Journal of Phycology*, 33,
603 368-376, doi:10.1111/j.0022-3646.1997.00368.x, 1997.
- 604 Karasiewicz S., Breton E., Lefebvre A., Farinas T. H. and Lefebvre S.: Realized niche analysis of
605 phytoplankton communities involving HAB: *Phaeocystis* spp. as a case study, *Harmful Algae*, 72,
606 1-13, doi:10.1016/j.hal.2017.12.005, 2018.
- 607 Kraus, Michael. Zur Bildung von TEP (transparent exopolymer particles) in der Kieler Bucht. Diss. Christian-
608 Albrechts-Universität zu Kiel, 1997.
- 609 Le Grix N., Zscheischler J., Laufkötter C., Rousseaux C. S. and Frölicher T. L.: Compound high-temperature
610 and low-chlorophyll extremes in the ocean over the satellite period, *Biogeosciences*, 18, 2119-2137,
611 doi:10.5194/bg-18-2119-2021, 2021.
- 612 Lee S. H., Kim B. K., Lim Y. J., et al. Lee S. H.: Small phytoplankton contribution to the standing stocks and
613 the total primary production in the Amundsen Sea, *Biogeosciences*, 14, 3705-3713, doi:10.5194/bg-
614 14-3705-2017, 2017.
- 615 Li Q. P., Zhou W., Chen Y. and Wu Z.: Phytoplankton response to a plume front in the northern South China
616 Sea, *Biogeosciences*, 15, 2551-2563, doi:10.5194/bg-15-2551-2018, 2018.
- 617 Li Y., Wang C., Liu H., Su J., Lan C. Q., Zhong M. and Hu X.: Production, isolation and bioactive estimation
618 of extracellular polysaccharides of green microalga *Neochloris oleoabundans*, *Algal Research*, 48,
619 101883, doi:10.1016/j.algal.2020.101883, 2020.



- 620 Li Y., Zhao J., Li D., et al. Zhang H.: Factors controlling the phytoplankton crops, taxonomic composition,
621 and particulate organic carbon stocks in the Cosmonaut Sea, East Antarctica, *Journal of Oceanology*
622 and *Limnology*, 1-14, doi:10.1007/s00343-024-3198-6, 2024.
- 623 Liu J., Lewitus A. J., Kempton J. W. and Wilde S. B.: The association of algicidal bacteria and raphidophyte
624 blooms in South Carolina brackish detention ponds, *Harmful Algae*, 7, 184-193,
625 doi:10.1016/j.hal.2007.07.001, 2008.
- 626 Mackey M., Mackey D., Higgins H. and Wright S.: CHEMTAX-a program for estimating class abundances
627 from chemical markers: application to HPLC measurements of phytoplankton, *Marine Ecology*
628 *Progress Series*, 144, 265-283, doi:10.3354/meps144265, 1996.
- 629 Magaletti E., Urbani R., Sist P., Ferrari C. R. and Cicero A. M.: Abundance and chemical characterization of
630 extracellular carbohydrates released by the marine diatom *Cylindrotheca fusiformis* under N-and P-
631 limitation, *European Journal of Phycology*, 39, 133-142, doi:10.1080/0967026042000202118, 2004.
- 632 Mari X. and Burd A.: Seasonal size spectra of transparent exopolymeric particles (TEP) in a coastal sea and
633 comparison with those predicted using coagulation theory, *Marine Ecology Progress Series*, 163,
634 63-76, doi:10.3354/meps163063, 1998.
- 635 Martinson D. G.: Antarctic circumpolar current's role in the Antarctic ice system: An overview,
636 *Palaeogeography, Palaeoclimatology, Palaeoecology*, 335, 71-74,
637 doi:10.1016/j.palaeo.2011.04.007, 2012.
- 638 Massolo S., Messa R., Rivaro P. and Leardi R.: Annual and spatial variations of chemical and physical
639 properties in the Ross Sea surface waters (Antarctica), *Continental Shelf Research*, 29, 2333-2344,
640 doi:10.1016/j.csr.2009.10.003, 2009.
- 641 Montgomery, Douglas C., Elizabeth A. Peck, and G. Geoffrey Vining. Introduction to linear regression
642 analysis. John Wiley & Sons, doi: 10.1080/02664763.2013.816069, 2021.
- 643 Moore C., Mills M., Arrigo K., et al. Jaccard S.: Processes and patterns of oceanic nutrient limitation, *Nature*
644 *Geoscience*, 6, 701-710, doi:10.1038/ngeo1765, 2013.
- 645 Mopper K., Zhou J. A., Ramana K. S., Passow U., Dam H. G. and Drapeau D. T.: The role of surface-active
646 carbohydrates in the flocculation of a diatom bloom in a mesocosm, *Deep-Sea Research Part II-*
647 *Topical Studies in Oceanography*, 42, 47-73, doi:10.1016/0967-0645(95)00004-a, 1995.
- 648 Noh K. M., Lim H.-G. and Kug J.-S.: Global chlorophyll responses to marine heatwaves in satellite ocean
649 color, *Environmental Research Letters*, 17, 064034, doi:10.1088/1748-9326/ac70ec, 2022.
- 650 Ortega-Retuerta E., Sala M. M., Borrull E., et al. Gasol J. M.: Horizontal and vertical distributions of
651 transparent exopolymer particles (TEP) in the NW Mediterranean Sea are linked to chlorophyll a
652 and O₂ variability, *Frontiers in Microbiology*, 7, doi:10.3389/fmicb.2016.02159, 2017.
- 653 Otero A. and Vincenzini M.: Extracellular polysaccharide synthesis by *Nostoc strains* as affected by N source
654 and light intensity, *Journal of Biotechnology*, 102, 143-152, doi:10.1016/s0168-1656(03)00022-1,
655 2003.
- 656 Pakhomov E.: Demography and life cycle of Antarctic krill, *Euphausia superba*, in the Indian sector of the
657 Southern Ocean: long-term comparison between coastal and open-ocean regions, *Canadian Journal*
658 *of Fisheries and Aquatic Sciences*, 57, 68-90, doi:10.1139/f00-175, 2000.



- 659 Park Y.-H., Charriaud E. and Fieux M.: Thermohaline structure of the Antarctic surface water/winter water
660 in the Indian sector of the Southern Ocean, *Journal of Marine Systems*, 17, 5-23,
661 doi:10.1016/S0924-7963(98)00026-8, 1998.
- 662 Passow U.: Formation of transparent exopolymer particles, TEP, from dissolved precursor material, *Marine*
663 *Ecology Progress Series*, 192, 1-11, doi:10.3354/meps192001, 2000.
- 664 Passow U.: Production of transparent exopolymer particles (TEP) by phyto- and bacterioplankton, *Marine*
665 *Ecology Progress Series*, 236, 1-12, doi:10.3354/meps236001, 2002a.
- 666 Passow U.: Transparent exopolymer particles (TEP) in aquatic environments, *Progress in Oceanography*, 55,
667 287-333, doi:10.1016/S0079-6611(02)00138-6, 2002b.
- 668 Passow U. and Alldredge A. L.: Distribution, size and bacterial colonization of transparent exopolymer
669 particles (TEP) in the ocean, *Marine Ecology Progress Series*, 113, 185-198,
670 doi:10.3354/meps113185, 1994.
- 671 Passow U. and Alldredge A. L.: Aggregation of a diatom bloom in a mesocosm: The role of transparent
672 exopolymer particles (TEP), *Deep-Sea Research Part II-Topical Studies in Oceanography*, 42, 99-
673 109, doi:10.1016/0967-0645(95)00006-c, 1995a.
- 674 Passow U. and Alldredge A. L.: A dye-binding assay for the spectrophotometric measurement of transparent
675 exopolymer particles (TEP), *Limnology and Oceanography*, 40, 1326-1335,
676 doi:10.4319/lo.1995.40.7.1326, 1995b.
- 677 Penna A., Berluti S., Penna N. and Magnani M.: Influence of nutrient ratios on the in vitro extracellular
678 polysaccharide production by marine diatoms from the Adriatic Sea, *Journal of Plankton Research*,
679 21, doi:10.1093/plankt/21.9.1681, 1999.
- 680 Price L., Yin K. and Harrison P.: Influence of continuous light and L: D cycles on the growth and chemical
681 composition of Prymnesiophyceae including coccolithophores, *Journal of Experimental Marine*
682 *Biology and Ecology*, 223, 223-234, doi:10.1016/S0022-0981(97)00168-8, 1998.
- 683 Radic T., Kraus R., Fuks D., Radic J. and Pecar O.: Transparent exopolymeric particles' distribution in the
684 northern Adriatic and their relation to microphytoplankton biomass and composition, *Science of the*
685 *Total Environment*, 353, 151-161, doi:10.1016/j.scitotenv.2005.09.013, 2005.
- 686 Ramaiah N., Yoshikawa T. and Furuya K.: Temporal variations in transparent exopolymer particles (TEP)
687 associated with a diatom spring bloom in a subarctic ria in Japan, *Marine Ecology Progress Series*,
688 79-88, doi:10.3354/meps212079, 2001.
- 689 Redfield A. C.: The biological control of chemical factors in the environment, *American scientist*, 46, 230A-
690 221, doi:<http://www.jstor.org/stable/27827150>, 1958.
- 691 Rivaro P., Messa R., Ianni C., Magi E. and Budillon G.: Distribution of total alkalinity and pH in the Ross
692 Sea (Antarctica) waters during austral summer 2008, *Polar Research*, 33, 20403,
693 doi:10.3402/polar.v33.20403, 2014.
- 694 Rousseau V., Vault D., Casotti R., Cariou V., Lenz J., Gunkel J. and Baumann M.: The life cycle of
695 Phaeocystis (Prymnesiophyceae): evidence and hypotheses, *Journal of Marine Systems*, 5, 23-39,
696 doi:10.1016/0924-7963(94)90014-0, 1994.
- 697 Schartau M., Engel A., Schröter J., Thoms S., Völker C. and Wolf-Gladrow D.: Modelling carbon
698 overconsumption and the formation of extracellular particulate organic carbon, *Biogeosciences*, 4,
699 433-454, 2007.



- 700 Smith D. C., Steward G. F., Long R. A. and Azam F.: Bacterial mediation of carbon fluxes during a diatom
701 bloom in a mesocosm, *Deep Sea Research Part II: Topical Studies in Oceanography*, 42, 75-97,
702 doi:10.1016/0967-0645(95)00005-b, 1995.
- 703 Staats N., Stal L. J. and Mur L. R.: Exopolysaccharide production by the epipelagic diatom *Cylindrotheca*
704 *closterium*: effects of nutrient conditions, *Journal of Experimental Marine Biology and Ecology*,
705 249, 13-27, doi:10.1016/s0022-0981(00)00166-0, 2000.
- 706 Tanioka T., Garcia C. A., Larkin A. A., Garcia N. S., Fagan A. J. and Martiny A. C.: Global patterns and
707 predictors of C: N: P in marine ecosystems, *Communications Earth & Environment*, 3, 271,
708 doi:10.1038/s43247-022-00603-6, 2022.
- 709 Tungaraza C., Rousseau V., Brion N., Lancelot C., Gichuki J., Baeyens W. and Goeyens L.: Contrasting
710 nitrogen uptake by diatom and Phaeocystis-dominated phytoplankton assemblages in the North Sea,
711 *Journal of Experimental Marine Biology and Ecology*, 292, 19-41, doi:10.1016/s0022-
712 0981(03)00145-x, 2003.
- 713 Van Boekel W., Hansen F., Riegman R. and Bak R.: Lysis-induced decline of a Phaeocystis spring bloom and
714 coupling with the microbial foodweb, *Marine Ecology Progress Series*, 269-276,
715 doi:10.3354/meps081269, 1992.
- 716 van Oijen T., van Leeuwe M. A. and Gieskes W. W.: Variation of particulate carbohydrate pools over time
717 and depth in a diatom-dominated plankton community at the Antarctic Polar Front, *Polar Biology*,
718 26, 195-201, doi:10.1007/s00300-002-0456-x, 2003.
- 719 Van Rijssel M., Janse I., Noordkamp D. and Gieskes W.: An inventory of factors that affect polysaccharide
720 production by *Phaeocystis globosa*, *Journal of Sea Research*, 43, 297-306, doi:10.1016/s1385-
721 1101(00)00013-7, 2000.
- 722 Waite A. M., Olson R. J., Dan H. G. and Passow U.: Sugar-containing compounds on the cell surfaces of
723 marine diatoms measured using concanavalin A and flow cytometry, *Journal of Phycology*, 31, 925-
724 933, doi:10.1111/j.0022-3646.1995.00925.x, 1995.
- 725 Williams G. D., Nicol S., Aoki S., Meijers A. J., Bindoff N. L., Iijima Y., Marsland S. J. and Klocker A.:
726 Surface oceanography of BROKE-West, along the Antarctic margin of the south-west Indian Ocean
727 (30–80°E), *Deep Sea Research Part II: Topical Studies in Oceanography*, 57, 738-757,
728 doi:10.1016/j.dsr2.2009.04.020, 2010.
- 729 Wright S. W., van den Enden R. L., Pearce I., Davidson A. T., Scott F. J. and Westwood K. J.: Phytoplankton
730 community structure and stocks in the Southern Ocean (30–80°E) determined by CHEMTAX
731 analysis of HPLC pigment signatures, *Deep Sea Research Part II: Topical Studies in Oceanography*,
732 57, 758-778, doi:10.1016/j.dsr2.2009.06.015, 2010.
- 733 Xu Q., Wang P., Huangleng J., et al. Jiang G.: Co-occurrence of chromophytic phytoplankton and the *Vibrio*
734 community during *Phaeocystis globosa* blooms in the Beibu Gulf, *Science of the Total Environment*,
735 805, 150303, doi:10.1016/j.scitotenv.2021.150303, 2022.
- 736 Xue T., Frenger I., Terhaar J., Prowe A. F., Frölicher T. L. and Oschlies A.: Southern Ocean phytoplankton
737 under climate change: shifting balance of bottom-up and top-down control, *Biogeosciences*, 2023,
738 1-27, doi:10.5194/bg-2023-171, 2023.



- 739 Yang Z., Liu Y., Ge J., Wang W., Chen Y. and Montagnes D.: Aggregate formation and polysaccharide content
740 of *Chlorella pyrenoidosa* Chick (Chlorophyta) in response to simulated nutrient stress, Bioresource
741 Technology, 101, 8336-8341, doi:10.1016/j.biortech.2010.06.022, 2010.
- 742 You T. and Barnett S. M.: Effect of light quality on production of extracellular polysaccharides and growth
743 rate of *Porphyridium cruentum*, Biochemical Engineering Journal, 19, 251-258, doi:10.1016/s1369-
744 703x(04)00028-2, 2004.
- 745 Zhan W., Zhang Y., He Q. and Zhan H.: Shifting responses of phytoplankton to atmospheric and oceanic
746 forcing in a prolonged marine heatwave, Limnology and Oceanography, 68, 1821-1834,
747 doi:10.1002/lno.12388, 2023.
- 748 Zhou J., Mopper K. and Passow U.: The role of surface-active carbohydrates in the formation of transparent
749 exopolymer particles by bubble adsorption of seawater, Limnology and Oceanography, 43, 1860-
750 1871, doi:10.4319/lno.1998.43.8.1860, 1998.
- 751